


Article

Forecasting Events in the Chaotic Dynamics of a Fiber Laser

Andrés Aragoneses ^{1,2} , Yingqi Ding ²

¹ Department of Physics, Eastern Washington University, Cheney, 99004, WA; aaragoneses@ewu.edu

² Department of Physics and Astronomy, Carleton College, Northfield, 55057, MN; dingy@carleton.edu

* Correspondence: aaragoneses@ewu.edu; Tel.: +1-509-359-7469

Abstract: Being able to forecast events is of great importance in many fields, from brain behavior to earthquakes or stock markets. Because each dynamical system has intrinsic features, different statistical tools have to be used for each system. Here we study the time series of the output intensity of a fiber laser with an ordinal patterns analysis, and we look for temporal correlations in order to statistically forecast the most intense events. We set two thresholds, a low one and a high one, to distinguish between low intensity versus high intensity events. We find that when the time series is performing events below the low threshold it shows some preferred temporal patterns before performing events above a high threshold.

Keywords: forecasting; complex dynamics; fiber laser; chaos; ordinal patterns.

1. Introduction

Time series analysis is a widespread research field that crosses disciplines. Nature presents many dynamical systems performing complex behavior that are only accessible through the temporal evolution of one or a few of its variables. Understanding the dynamical behavior relies on finding characteristic features that allow us to classify them and make predictions about their immediate future, based on their present demeanor [1–12]. Complex systems constitute a challenge, as the nonlinear interplay between the numerous elements of the system, the presence of time delay, and noise make them impractical for a bottom-up analysis.

Lasers constitute a great example of a dynamical system performing complex behavior. Besides the innumerable technological applications, lasers are a fascinating tool for the study and characterization of nonlinear dynamics from a laboratory-controlled manner [13].

One particular case of laser manifesting complex dynamics are fiber lasers with optical feedback [14]. In previous studies [15,16] it was found that behind the high complexity of the time series of the output intensity of a fiber laser, the system showed some structure that could be unveiled using an ordinal patterns analysis. It was found that the laser executes some preferred intensity and temporal patterns, and those patterns helped to detect a laminar to turbulent transition as the pump power of the laser was increased [14,15]. In Ref. [16], through a simple mathematical model and an ordinal patterns analysis, it was also seen that the transition was related to internal frequencies of the dynamics. In this paper we use the ordinal patterns analysis to study the complex behavior of the output intensity of the fiber laser, to forecast when the laser is changing from emitting low intensity to emit high intensity light.

2. Forecasting method

The ordinal patterns analysis method (OPAM) introduced by Bandt and Pompe in 2012 [17] studies correlations between consecutive events. It defines patterns by comparing the values of n consecutive events in a time series (either magnitudes or time intervals between events), and computes the probabilities of each of the $n!$ possible patterns. For a purely stochastic process, where no correlations exist between events, one would expect to find all patterns equally probable ($P = 1/n!$),

while for systems that present some intensity or temporal correlation one would expect some structure in the probabilities of the patterns. This method has been used to characterize complex dynamics based on the patterns probabilities [9,12,18,19], to distinguish between stochasticity and determinism [20], or to identify transitions in the dynamics of complex networks [21]. In a recent paper [22] the method was used to classify events into two types, and to forecast when the system decides to change from one type of events to the other one.

The OPAM transforms the original series of m events, $X = \{x_1, x_2, \dots, x_i, \dots\}$, into a series of $m - n$ patterns. To do so, it considers n consecutive events, assigns them correlative integer numbers (0, 1, 2, ..., n), and then orders them from smaller to larger value of the event. For example for dimension $n = 2$, if $x_i < x_{i+1}$, it labels that pattern as 01, if $x_{i+1} < x_i$, it labels that pattern as 10. For dimension $n = 3$ we have six possible patterns (012, 021, 102, 120, 201, 210), i.e., if $x_i < x_{i+1} < x_{i+2}$ it labels that pattern as 012; $x_i < x_{i+2} < x_{i+1}$ is 021 ...

This can be applied to the actual values of the events ($\{x(i)\}$), the magnitudes in the time series, but it can also be applied to the time intervals between events ($\{t(i+1) - t(i)\}$). The former would give us information about intensity correlations among consecutive events, while the latter about temporal correlations.

For the fiber laser under study both, intensity and temporal correlations were found (see Fig. 2a,b from Ref. [15]), where some patterns were more likely to happen in the time series. The fact that the OPs are not equally probable means that the dynamics is not compatible with a stochastic process, but it is clearly deterministic. The system showed a higher degree of determinism at the laminar-turbulent transition.

3. Results

We analyze the output intensity of a fiber laser with optical feedback. Time series are recorded for 625 ms, with 5×10^7 points and $\Delta t = 12.5$ ps. The time series are recorded for output powers between 0.80 W and 1.50 W (see Ref. [14] for details). The time series are subtracted the average and normalized to the standard deviation. We detect the peaks in the time series as events and study the time series of these events.

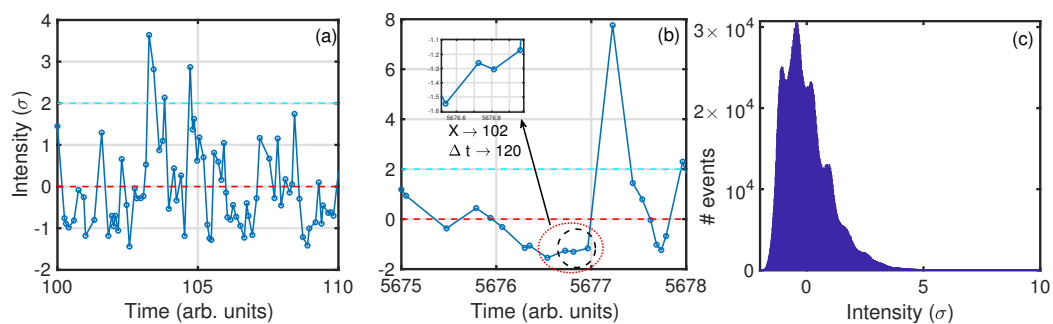


Figure 1. (a) Time series of the events that oscillate around 0 but that present some intensity events larger 2σ . Two thresholds are depicted, a low one at the mean value of the intensities, $th_0 = 0$, and a high one at $th^* = 2\sigma$. (b) Detail of the time series where four events are selected, below th_0 that precede a high intensity event, above th^* . The dotted red circle and the dashed black circle indicate the four (three) consecutive events below th_0 used to generate an OP. Three consecutive events when OPs are computed with intensities, and four consecutive events when OPs are computed. (c) Histogram of events for power of 1.20 W. The distribution of events shows some structure and a tail that reaches values larger than 6σ .

Figure 1a shows a section of a time series of events. The time series of the output intensity shows a wide distribution with most values around $\pm 2\sigma$ and fewer events reaching values $> 6\sigma$. The insert in Fig. 1b shows four consecutive events and the corresponding OP generated. The black circle in Fig. 1b indicates the three events considered to generate the OP with intensity of the values

($X_{i+1} > X_i > X_{i+2} \rightarrow 102$), and the red circle indicates the four consecutive events considered to generate the OP with their inter-event time-intervals ($\Delta t_{i+1} < \Delta t_{i+2} < \Delta t_i \rightarrow 120$).

Figure 1c shows the histogram of the intensity for 1.00 W. This histogram shows a long tail for high intensities. This type of long-tail distribution is present in a wide variety of systems [23–26], that can lead to unwanted phenomena. Hence the importance of understanding and being able to forecast when the system is going to perform events corresponding to the tail, sometimes referred to as extreme events.

We define a threshold, th^* , to classify the events as large, or extreme, when they are above that threshold. We are interested in predicting when the system changes from emitting low intensity light (lower than th^*) to emit high intensity light (higher than th^*).

To forecast the change from low intensity behavior to high intensity one, we impose that at least three consecutive events are below th^* before the system goes to emit a high intensity event (see figure 1b). We compute the ordinal patterns (OPs) of the three inter-event time-intervals right before the system changes from low to high intensity. This will indicate if there are OPs that are more/less likely to happen before the transition, and which OPs these are.

Figure 2 shows the six OPs of dimension three versus the threshold, th^* , for three power outputs, $P = 0.80$ W (below laminar to turbulent transition), $P = 0.90$ W (at the transition), and $P = 1.10$ W (after the transition). The top row corresponds to the OPS generated with the intensity of the events. It can be observed that there are OPs that are more likely to happen and OPs that are less likely to happen, before the transition from low to high intensity. This points to some structure in the complex dynamics that manifests as a preference of patterns before performing a high intensity event. The gray region corresponds to the probabilities of a stochastic process of the six OPs equally probable. This region depends on the number of events in each threshold. For high enough threshold the number of high intensity events preceded by low intensity events is too low to have conclusive statistics, and therefore the OPs probabilities lie in the gray region.

The second row in Fig. 2 groups the six OPs into three, depending on the last event, to highlight this last event (the event preceding the high intensity event) with respect to the previous two ($XX0 = 120 + 210$, the latter event is smaller than the previous two; $XX1 = 021 + 201$, the latter event is intermediate; $XX2 = 012 + 102$, the latter event is larger than the previous two). This indicates that between 40% and 50% of the high intensity events will be preceded by pattern $XX2$, i.e., of the three preceding events, the latest one is higher than the other two. In other words this indicates that the change from low intensity to high intensity is not as sharp as it could be. This figure also shows that the OPs probabilities do not depend on the threshold.

The bottom row shows the OPs generated with inter-event time-intervals. For low thresholds, th^* , the probabilities are not compatible with a stochastic process but they are much smaller than the ones computed with intensities. This shows that the dynamics presents less intense temporal correlations than correlations in magnitude. Also, the hierarchy is different from the top to the bottom row. Also in a previous work [15] were found temporal correlations of less relevance than intensity correlations.

There is little effect of the power output of the laser on the probabilities of the OPs. For the intensity OPs, the more likely OPs are more probable and the less likely OPs are less probable at the transition power (0.80 W), while for the temporal OPs, all are more equally probable, lying on or very near the gray region.

Splitting the peaks into above and below a single threshold does not separate events into those that are much larger than average (events that can be considered as extreme events) and those events around and below average. In Fig. 3 we consider two thresholds, a low one, th_0 , and a high one, th^* . We set the lower threshold at $th_0 = 1\sigma$ and scan the high threshold, $2 \leq th^* \leq 4$. We then calculate the OPs probabilities, (see Fig. 3).

We find that there are still preferred patterns before jumping from below th_0 to above th^* . The preferred OPs are the same as in Fig. 2. This is interesting as the conditions to select the events to build the OPs are not the same. In the first case it was less restrictive, and low events could be very close

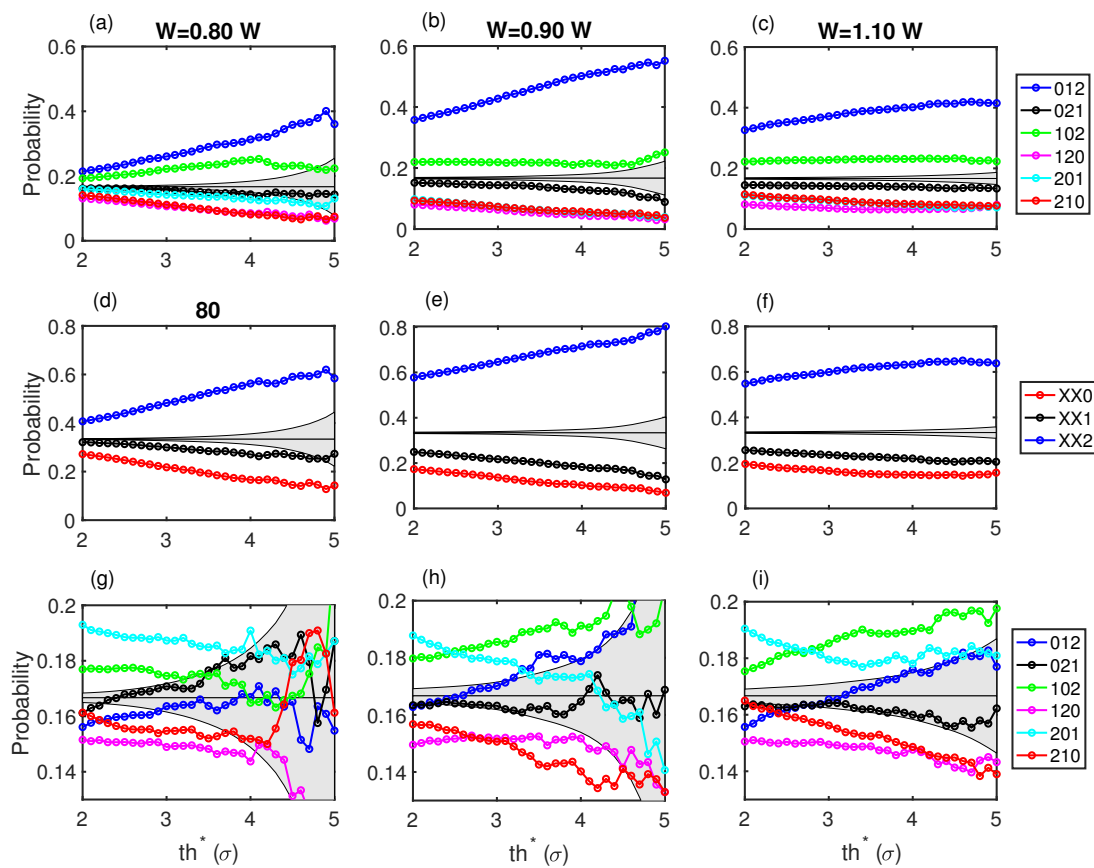


Figure 2. (a-c) Ordinal patterns computed with intensities. Three consecutive events below th^* , that precede an event above th^* are considered for each OP. (d-f) The OPs are grouped into $XX0 = 120 + 210$, $XX1 = 021 + 201$, and $XX2 = 012 + 102$. This highlights the fact that the most likely OPs to happen before a jump from low intensity events to high intensity event are those where the last event is larger than the previous two. (g-i) OPs computed with inter-event time-intervals. The gray region corresponds to a stochastic process where all six patterns are equally probable.

118 to th^* , while in the second case all events that contribute to the OP are below th_0 . This suggests that
 119 when the low events are near the low threshold, th_0 , there is more chance for a high event to happen.

120 With this more restrictive condition of two thresholds the number of events that satisfy that
 121 $x_{i-3} < th_0$, $x_{i-2} < th_0$, $x_{i-1} < th_0$, and $x_i > th^*$ is reduced. This is reflected in the wider gray regions
 122 in Fig. 3, and in the fact that above $th^* = 4\sigma$ the probabilities are compatible with a stochastic process,
 123 so we cannot use this as a forecasting method. In any case, for power outputs of the laser above the
 124 transition ($P \geq 0.90 W$), and events larger than 3.5σ , we can still see that 50% of these intense events
 125 happen after the XX2 pattern.

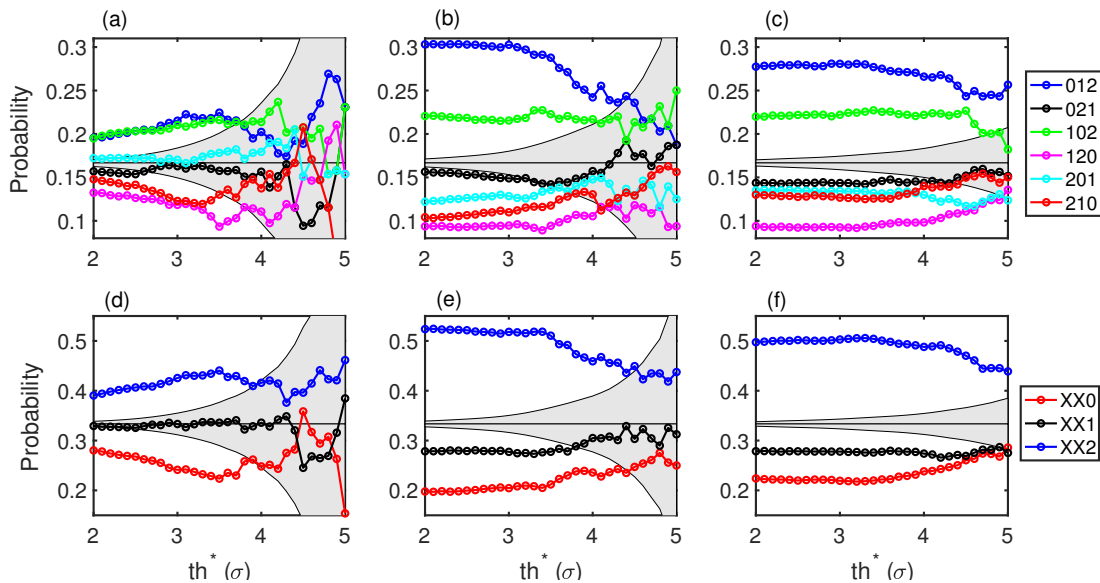


Figure 3. Ordinal patterns computed with intensities using two thresholds. A low threshold, $th_0 = 1\sigma$, imposes that the consecutive low events that form OPs are below th_0 . A high threshold selects the high events that take place after the OP and are above $2\sigma \leq th^* \leq 4\sigma$. (a-c) Correspond to the six OPs of dimension three. (d-f) correspond to the OPs combinations where the last of the three event is larger, in between, or shorter than the other two events. This more restrictive condition reduces the number of events and widens the gray area.

126 4. Conclusions

127 We have studied the dynamics of the output light of a fiber laser with optical feedback. By using
 128 an ordinal patterns approach, we have found signatures of determinism in its dynamics that allow us
 129 to forecast extreme events, defined as events larger than a threshold ($th^* > 2\sigma$). The system presents
 130 preferred patterns before it changes from low intensity events to more extreme events. The preferred
 131 pattern before an extreme event is the one where the latter of three consecutive events below the
 132 threshold is larger than the previous two, with probabilities that reach 80% in some cases, while the
 133 less probable pattern is the one where the latter event is less intense than the previous two events,
 134 which in some cases reaches less than 10%.

135 We can compute the patterns with the intensity of the events or with the inter-event time-intervals.
 136 The former takes advantage of intensity correlations in the system while the latter on temporal
 137 correlations, both of them present in the dynamics. In this system the more efficient way to compute
 138 the patterns for forecasting purposes is with the actual intensity of the events. For patterns computed
 139 with inter-event time-intervals the probabilities, although still not compatible with a stochastic process,
 140 are lower and therefore less efficient to forecast the more extreme events.

141 The fact that there is 70% higher probability of pattern XX2 before a sudden increase in intensity
 142 has to be considered carefully, as there are much less events that are higher than th^* than events below

143 th_0 . This means that not after 70% of all patterns XX2 in the time series will take place an extreme
 144 event, but that 70% of extreme events are preceded by pattern XX2.

145 One interpretation for this preference for specific patterns when the system leaves the low intensity
 146 regime and explores the higher intensity regime is that there is a specific region in phase space that
 147 triggers extreme events, and those patterns are the signature of that region in phase space.

148 This methodology can be applied to other complex dynamical systems that manifest time series
 149 of events, with a long-tail histogram.

150 **Author Contributions:** Y. D. analyzed the data, A. A. wrote the manuscript. Y. D. and A. A. discussed the results
 151 and revised the manuscript.

152 **Funding:** This work was supported in part by Carleton College Towsley Endowment.

153 **Acknowledgments:** The authors thank N. Tarasov, D. V. Churkin, and S. K. Turitsyn for the experimental data.

154 **Conflicts of Interest:** The authors declare no conflict of interest.

155 References

- 156 1. Robert J. Geller, David D. Jackson, Yan Y. Kagan, and Francesco Mulargia, Earthquakes Cannot Be Predicted.
 157 *Science* **1997**, *275*, 3506, 1616.
- 158 2. Álvaro Corral, Long-Term Clustering, Scaling, and Universality in the Temporal Occurrence of Earthquakes.
 159 *Phys. Rev. Lett.* **2004**, *92*, 10, 108501.
- 160 3. Yan Y. Kagan, Worldwide earthquake forecasts. *Stoch. Environ. Res. Risk Assess.* **2017**, *6*, 1273-1290.
- 161 4. Álvaro Corral, Josep Sardanyés, and Lluís Alsedà, Finite-time scaling in local bifurcations. *Scientific Reports*
 162 **2018**, *8*, 11783.
- 163 5. Alexander B. Neiman, and David F. Russell, Models of stochastic biperiodic oscillations and extended serial
 164 correlations in electroreceptors of paddlefish. *Phys. Rev. E* **71**, 061915 (2005).
- 165 6. Belén San Cristóbal, Beatriz Rebollo, Pol Boada, Maria V. Sánchez-Vives, and Jordi García-Ojalvo. Collective
 166 stochastic coherence in recurrent neuronal networks. *Nat. Physics* **2016**, *12*, 881-888.
- 167 7. Vasyly Palchykov, Marija Mitrovic, Hang-Hyun Jo, Jari Saramäki, and Raj Kumar Pan. Inferring human
 168 mobility using communication patterns. *Scientific Reports* **2014**, *4*, 6174.
- 169 8. C.-K. Peng, J. Mietus, J. M. Hausdorff, S. Havlin, H. E. Stanley, and A. L. Goldberger. Long-Range
 170 Anticorrelations and Non-Gaussian Behavior of the Heartbeat. *Phys. Rev. Lett.* **1993**, *70*, 9, 1343-1346.
- 171 9. U. Parlitz, S. Berg, S. Luther, A. Schirdewan, J. Kurths, N. Wessel. Classifying cardiac biosignals using ordinal
 172 pattern statistics and symbolic dynamics. *Comput. Biol. Med.* **2012**, *42*, 319-327.
- 173 10. Massimiliano Zanin, Luciano Zunino, Osvaldo A. Rosso, and David Papo, Permutation Entropy and Its
 174 Main Biomedical and Econophysics Applications: A Review. *Entropy* **2012**, *14*, 1553-1577.
- 175 11. Miguel C. Soriano, Jordi García-Ojalvo, Claudio R. Mirasso, and Ingo Fischer Complex photonics: Dynamics
 176 and applications of delay-coupled semiconductor lasers. *Rev. Mod. Phys.* **2013**, *85*, 421(50).
- 177 12. Luciano Zunino, Massimiliano Zanin, Benjamin M. Tabak, Darío G. Pérez, Osvaldo A. Rosso. Forbidden
 178 patterns, permutation entropy and stock market inefficiency. *Physica* **2009**, *388*, 2854-2864.
- 179 13. Miguel C. Soriano, Jordi García-Ojalvo, Claudio R. Mirasso and Ingo Fischer. Complex photonics: Dynamics
 180 and applications of delay-coupled semiconductor lasers. *Rev. Mod. Phys.* **2013**, *85*, 412.
- 181 14. E. G. Turitsyna, S. V. Smirnov, S. Sugavanam, N. Tarasov, X. Shu, S. A. Babin, E. V. Podivilov, D. V. Churkin,
 182 G. E. Falkovich, and S. K. Turitsyn. The laminar-turbulent transition in a fibre laser. *Nat. Photonics* **2013**, *7*,
 183 783, 2864.
- 184 15. Andrés Aragonés, L. Carpi, N. Tarasov, D. V. Churkin, M. C. Torrent, C. Masoller, and S. K. Turitsyn. *Phys.*
 185 *Rev. Lett* **2016**, *116*, 033902.
- 186 16. L. Carpi and C. Masoller. Persistence and stochastic periodicity in the intensity dynamics of a fiber laser
 187 during the transition to optical turbulence. *Phys. Rev. A* **2017**, *97*, 023842.
- 188 17. J. M. Amigo, K. Keller, and J. Kurths, Recent progress in symbolic dynamics and permutation complexity:
 189 ten years of permutation entropy. *Eur. Phys. J. Spec. Top.* **2013**, *222*, 2.

- 190 18. O.A. Rosso, and C. Masoller. Detecting and quantifying temporal correlations in stochastic resonance via
191 information theory measures. *Eur. Phys. J. B*, **2009**, 69, 37-43.
- 192 19. Max L. Trostel, Moses Z. R. Mispion, Andrés Aragoneses, and Arjendu K. Pattanayak. Characterizing
193 Complex Dynamics in the Classical and Semi-Classical Duffing Oscillator Using Ordinal Patterns Analysis.
194 *Entropy*, **2018**, 20, 40.
- 195 20. Andrés Aragoneses, Nicolás Rubido, Jordi Tiana-Alsina, M. C. Torrent, and Cristina Masoller, Distinguishing
196 signatures of determinism and stochasticity in spiking complex systems. *Scientific Reports* **2013**, 3, 1778.
- 197 21. Jiayang Zhang, Jie Zhou, Ming Tang, Heng Guo, Michael Small, and Yong Zou, Constructing ordinal
198 partition transition networks from multivariate time series. *Scientific Reports* **2017**, 7, 7795.
- 199 22. Meritxell Colet and Andrés Aragoneses, Forecasting Events in the Complex Dynamics of a Semiconductor
200 Laser with Optical Feedback. *Scientific Reports* **2018**, 8 10741.
- 201 23. Hugo L. D. de S. Cavalcante, Marcos Oria, Didier Sornette, Edward Ott, and Daniel J. Gauthier. Predictability
202 and Suppression of Extreme Events in a Chaotic System. *Phys. Rev. Lett.* **2013**, 111, 198701.
- 203 24. Alexander N. Pisarchik, Rider Jaimes-Reátegui, Ricardo Sevilla-Escoboza, G. Huerta-Cuellar, and Majid Taki.
204 Rogue Waves in a Multistable System. *Phys. Rev. Lett.* **2017**, 107, 274101.
- 205 25. Jordi Zamora-Munt, Bruno Garbin, Stephane Barland, Massimo Giudici, Jose R. Rios Leite, Cristina Masoller,
206 and Jorge R. Tredicce. Rogue waves in optically injected lasers: Origin, predictability, and suppression. *Phys.*
207 *Rev. Lett.* **2013**, 87, 035802.
- 208 26. Tian Jin, Chen Siyu, and Cristina Masoller. Generation of extreme pulses on demand in semiconductor lasers
209 with optical injection. *Opt. Expr.* **2017**, 35, 31326.